THE USE OF NOVEL DIMENSION REDUCTION OPTICAL FIBER ARRAYS FOR HYPERSPECTRAL IMAGING IN FLAMES

Rosemarie C. Chinni, Maria V. Schiza, and S. Michael Angel*
Department of Chemistry and Biochemistry
University of South Carolina Columbia, SC 29208

ABSTRACT

We are investigating a new approach to hyperspectral imaging that is well suited to simultaneous measurements of temperature and fluorescent species, such as the OH radical, in a flame or other combustion system. In this technique, the flame region of interest is imaged onto the tip of an optical fiber array that contains 500-600 fibers. The image is then transformed at the other end into a linear array and is re-imaged onto the vertical slit of a high-resolution spectrograph. The light from each fiber in the array is spectrally dispersed and all fiber spectra are simultaneously measured using an intensified CCD. Spectral images are then reconstructed at any wavelength, or combination of wavelengths, to show the distribution of temperature or species concentrations in the flame. It is shown that a single measurement of this type can yield data on the two-dimensional distribution of temperature and the relative concentration distribution of a variety of species in a flame. In this paper, we show feasibility by measuring flame temperature and emission of reference species. In a related study, we are investigating laser ablation to introduce controlled amounts of flame retardant chemicals into a flame.

Key words: Fiber-optic sensor, dimension reduction fiber array, flame temperature distribution, flame retardants, laser ablation

1. INTRODUCTION

Hyperspectral imaging involves the measurement of spectral images, *e.g.* fluorescence and emission, simultaneously in many different spectral regions. Spectral images are normally attained by the use of a 2-dimensional (2-D) detector such as a CCD or ICCD (charged coupled device or intensified charged coupled device), this is essentially a single wavelength technique. When several species or emission wavelengths need to be imaged, separate images must be taken at each wavelength of interest. This drawback led to the development of dimension reduction arrays. These arrays were first developed in the mid 1980's for stellar emission studies[1] and have been widely used in astronomical spectral imaging.[2-7] This approach has now been extended for analytical uses. Recent research by Ben-Amotz and co-workers includes micro-Raman, NIR-Raman, absorption, and fluorescence imaging using fiber-optic dimension reduction.[8-10]

Basically, this technique incorporates a fiber bundle in which the fibers are arranged 2-dimensionally at the input end and vertically (1-dimensionally) at the output end. By imaging the 1-D side of the array onto the slit of a spectrograph and recording the image with a 2-D detector, high spectral resolution can be attained at many spectral

wavelengths simultaneously in one image.[11] The advantages of this technique include very high spectral resolution and simultaneous imaging at many wavelengths. The spatial resolution using this technique is limited by the number of fibers in the array and ultimately by the height of the CCD or ICCD detector.

Recently, Myrick et. al. have developed a dimension reduction fiber array consisting of approximately 600, square, f/2 fibers.[12] His group used the array imaging a laser-induced plasma.[13,14] Recently, our group has used this type of array to detect multiple analytes using a combination CO_2/O_2 sensor.[15-17] In this paper, we report the first use of a dimension reduction fiber array to map the temperature distribution of an acetylene flame. We propose to use this technique to measure the effect of flame retardant chemicals on energetic radical flame species.

2. EXPERIMENTAL

2.1 Burner Slot Assembly

A six inch slot burner that was taken from an atomic absorption (AA) spectrometer (Perkin-Elmer model 303-011) was used for these measurements. Acetylene is connected to the fuel valve of the burner and air is connected to the nebulizer. Air serves as both the flame oxidizer and the nebulizing gas. Depending on the experiment, water, Fe standard (VWR Scientfic Products, 10,000 ppm), or solutions of ferrocene (Aldrich) and HBCD (hexabromocyclododecane, flame retardant) dissolved in toluene were aspirated into the flame at a rate of 2.73 mL/min.

2.2 Laser Ablation/LIF system

The experimental arrangement for LIF of •OH is shown in Figure 1. In this setup, the frequency doubled output of a Nd:YAG laser is used to pump a frequency doubled dye laser (Continuum Model Nd6000) emitting approximately 3.5 mJ/10 ns pulse at 281.10 nm. This wavelength corresponds to the energy of the $A^2\Sigma^+ \rightarrow X^2\pi$ transition of •OH. The laser beam is focused to a point on the front edge of the six-inch slot burner with a 200 mm focal length plano convex lens. This supplies sufficient power to allow for saturation of the •OH in the flame.

A Nd:YAG laser (New Wave, Model MiniLase-10) was used to ablate material from the polymer plaques into the flame. The resulting•OH fluorescence is collected by a 100 mm focal length lens and focused onto the slit of a 0.85 m double monochromator (SPEX model 1404) set to monitor the 314.58 nm •OH emission. The spectrometer resolution was approximately 0.012 nm. A photomultiplier tube (PMT) (Hammamatsu Model R2949) was used to monitor the signal, the output of which was connected directly to a 500 MHz digital sampling oscilloscope. Five trials were taken for each polymer plaque.

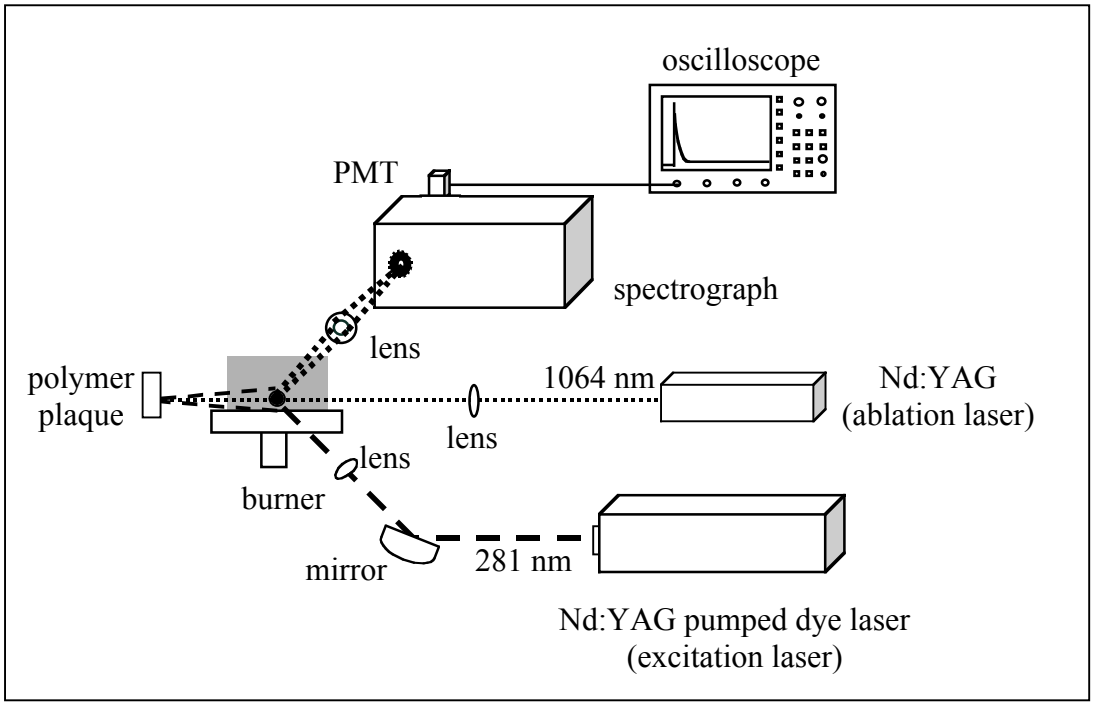

Figure 1. Schematic of the laser ablation/laser-induced fluorescence set-up.

2.3 Imaging System With the Dimension Reduction Fiber Array

A schematic of the imaging system is shown in Figure 2. The imaging system consists of a spectrometer (0.5 M Spex, Model No. 1870) with a 1200 grooves/mm grating and a 576 x 384 intensified charged coupled device (ICCD) detector (Princeton Instruments Inc., Model ITEA/CCD-576-S/RB-E). Two lenses are used to focus a 5x5 mm area of the flame onto the 2-D side of the dimension reduction fiber array. Two lenses are used to focus the 1-D side of the fiber array onto the slit (70 um) of the spectrometer. The fiber array is constructed of 608 square f/2 optical fibers (Collimated Holes Inc.) It consists of 19 ribbons that contain 32 square fibers each (19x32 matrix at the 2-D side, all of the ribbons are aligned vertically at the 1-D side of the fiber array). All of the spectral images were taken by using a 1 s exposure time with 500 accumulations.

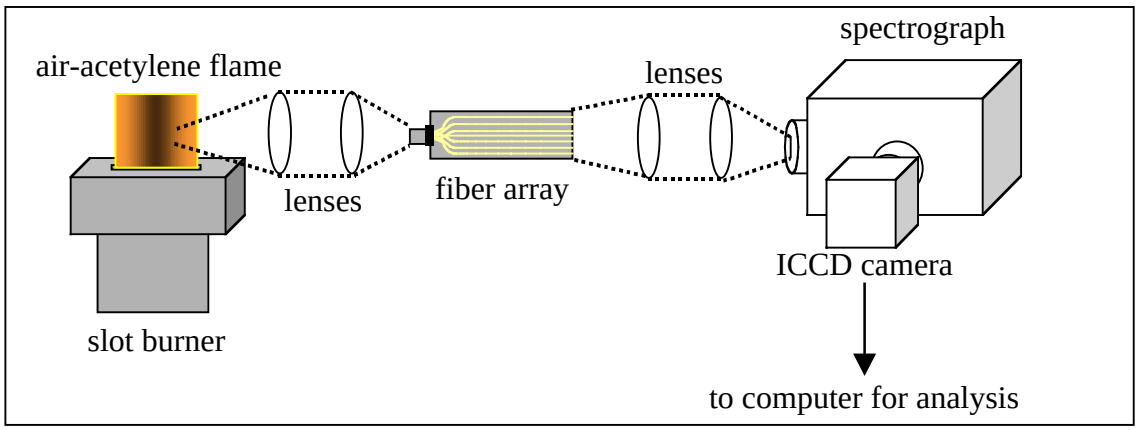

Figure 2. Schematic of the imaging set-up with the dimension reduction fiber array.

2.4 Data Analysis

All of the spectral images were worked up in IPLab Version 3.5.2 (Scanalytics, Inc.) and Igor Pro 3.16 (WaveMetrics, Inc.). An Igor Pro macro was used to calculate the temperature distributions using the Boltzmann equation (Equation 1):

$$\ln(I_{kj}\lambda_{kj}/g_kA_{kj}) = -E_k/k_bT + \ln(N(T)/u(T));$$

where I_k is the intensity of the transition, λ_k is the wavelength used, g_k is the statistical weight, A_{kj} is the probability that the transition will occur, E_k is the upper energy for that transition, k_b is the Boltzmann constant, T is the temperature in kelvin, N(T) is the number density, and u(T) is the partition function. The temperature is calculated without knowledge of the partition function and number density. The left-side of the equation is plotted against the Upper Energies. The slope (m) is equal to $1/k_bT$ and a linear plot yields the excitation temperature. Five trials were taken for each set of data. All of the error bars shown represent ± 1 standard deviation.

3. RESULTS AND DISCUSSION

3.1 Laser Ablation/LIF Results

In these measurements the polymer plaque is placed about 20 mm from the flame; any closer and the heat from the flame begins to melt the plaques. The laser was operated at 10 Hz to allow one pulse of the laser to ablate the particles into the flame and the next subsequent pulse of the dye laser to excite the •OH present in the flame. Since the particles remain for several hundred milliseconds, a high concentration of particles were still present in the flame upon arrival of the second laser pulse. When the sample position was determined to be optimal, •OH LIF data was obtained for the ablation process. When the ABS (polymer) plaques containing various concentrations of XP-2000 (flame retardant) were ablated into the flame, there was a noticeable effect on •OH concentrations (Figure 3). In this case, the maximum decrease in •OH LIF is approximately 55 %. The ratio of the signal of polymer plaques with flame retardants to the signal of pure polymer only (total •OH concentration) is called the relative decrease

in •OH concentration. These results are similar to those obtained when the flame retardant is dissolved and nebulized. Thus, these experiments show that laser ablation is a valid technique for sample introduction of non-soluble polymers. An advantage to using laser ablation for introducing polymer plaques into the flame is that the burner does not need to be shut off and cleaned every few minutes due to clogging from the sample as with aspirating the sample into the flame. Furthermore, most of the polymer plaques are very difficult to dissolve.

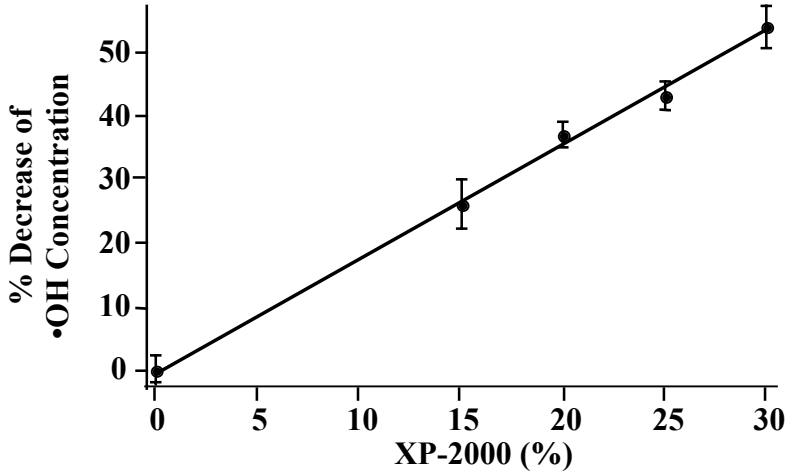

Figure 3. Relative decrease of the •OH concentration upon the introduction of the polymer plaques.

3.2 Temperature Imaging

One of the main purposes of this paper is to demonstrate the use of the dimension reduction fiber array to measure temperatures in flames over many different points simultaneously. A 5x5 mm area of the flame was imaged onto the 2-D side of the fiber array. The 1-D side of the fiber array was focused onto the entrance slit of a spectrometer, spectrally dispersed, and recorded with an ICCD detector. A typical image acquired from the ICCD detector with its corresponding spectrum can be seen in Figures 4 a and b. Note each image contains 608 complete spectra.

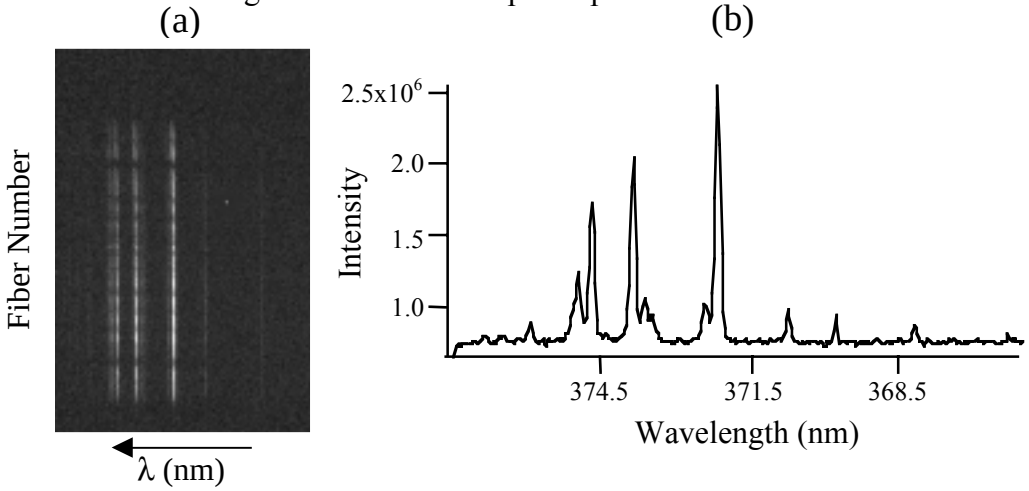

Figure 4. A typical image (a) recorded with the ICCD detector with its corresponding spectrum (b). The spectral lines shown in the image represent Fe lines. The spectrum here was obtained by averaging over the entire image.

Iron emission is commonly used to determine the excitation temperatures of a flame. To test the fiber array imaging technique, we measured the iron emission lines as ferrocene solutions were aspirated into the flame with and without flame retardant HBCD.

Temperature distributions were measured three different ways: full area temperature average, a vertical temperature profile, and a 2-D temperature profile. Initially, the entire image was averaged to obtain a spectral profile indicating the average flame temperature. A Boltzmann plot was performed using the Fe spectral lines in the region of 370-380 nm. The temperatures averaged over the entire areas with and without flame retardant were 2081±37 K and 2299±47 K, respectively. The results show that the temperature of the flame decreased significantly, as expected, upon the addition of flame retardant. This is due to the ability of the flame retardant to inhibit combustion in the flame thus lowering the temperature.

Next, the signal from the pixel in the ICCD image were added together (*i.e.*, "binned") to obtain the complete spectra from each of the 19 ribbons on the 1-D side of the array, simultaneously. These 19 spectra were used to determine a vertical temperature profile. Again , a Boltzmann plot was performed on each ribbon using the Fe spectral lines in the region of 370-380 nm. A graph comparing the temperature results from the images taken with and without flame retardant can be seen in Figure 5. The average temperatures across all 19 ribbons were 2091±39 K and 2317±31 K with and without flame retardant, respectively. These results agree with the previous results showing that addition of flame retardant decreases the temperature significantly.

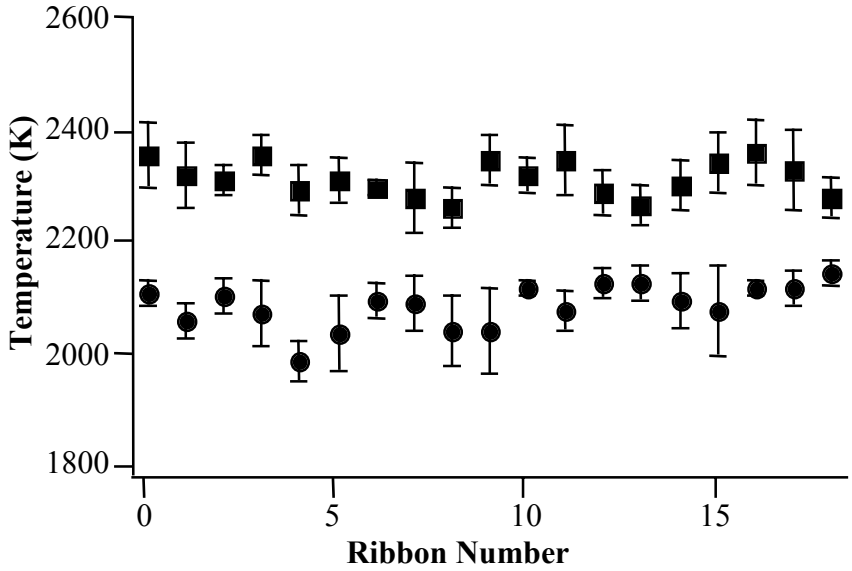

Figure 5. Comparison of temperatures calculated after binning each fiber ribbon individually on the 1-D side of the fiber array. Squares (■) represent temperatures calculated with no flame retardant and circles (●) represent temperatures calculated with flame retardant. This shows thr vertical temperature distribution.

Lastly, complete spectra were measure for each fiber in the array. That is, the entire ICCD image was used to calculate Boltzmann temperatures for each fiber (608 total) on the 2-D side of the array, corresponding to a different position in the flame. These spectral images were then used to construct "maps" showing the temperature

distribution in the flame. The temperature distributions for the flame with and without flame retardant are shown in contour plots (Figures 6a and 6b, respectively). The average temperatures across the imaged area were 2148±148 K and 2315±107 K with and without flame retardant, respectively. The results for the temperature distribution are in agreement with both the vertical temperature profile and whole image temperature average.

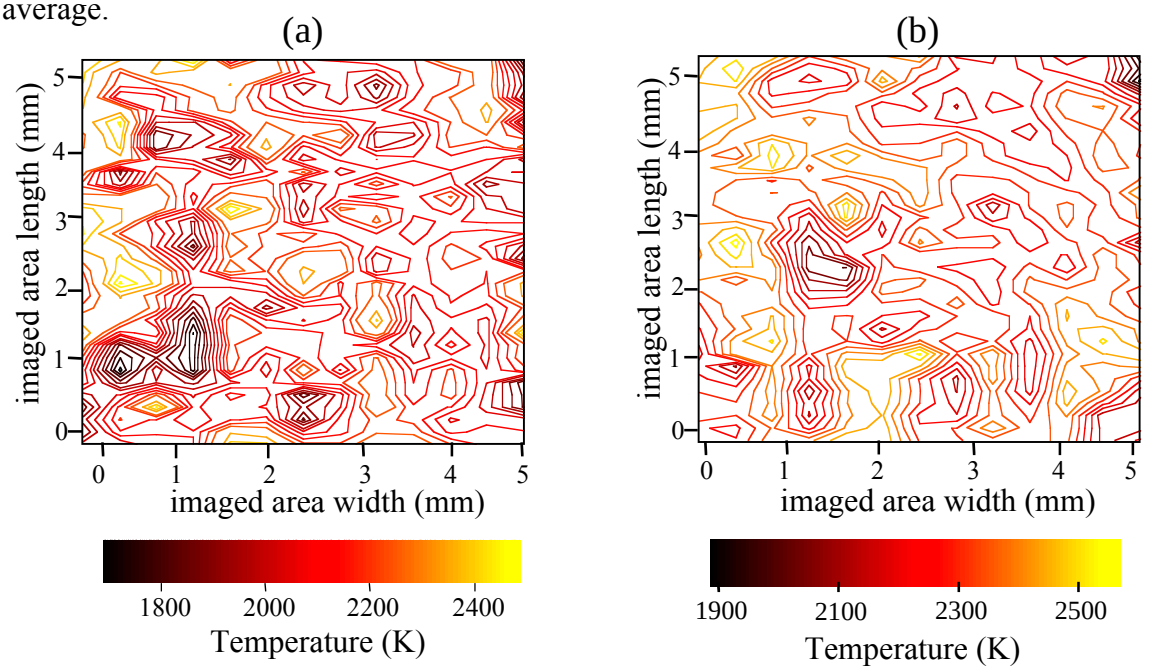

Figure 6 (a) Temperature distribution of the acetylene flame with flame retardant (HBCD) (b) Temperature distribution of the acetylene flame without flame retardant.

Temperatures were also measured in acetylene-rich and acetylene-deficient flames in order to change the overall flame temperature. For this data, the flame was aspirated with a standard Fe solution. To produce an acetylene-deficient flame the air pressure was held constant while the acetylene pressure was slightly lowered.

The temperatures calculated over the entire images were 2278±44 K and 2057±18 K for the acetylene-rich and acetylene-deficient flames, respectively. As expected, the results show that the temperature measured for the acetylene-rich flame is significantly higher than the temperature measured for the acetylene-deficient flame.

Again, the temperatures were calculated for each ribbon of 1-D side of the array with the data taken for an acetylene-rich flame and an acetylene-deficient flame. A graph comparing the temperature results from the images taken for this data can be seen in Figure 7. This shows the vertical temperature distribution. The average temperatures across all 19 ribbons were 2284±30 K and 2035±26 K for acetylene-rich and acetylene-deficient flames, respectively. These results also agree with the averaged results.

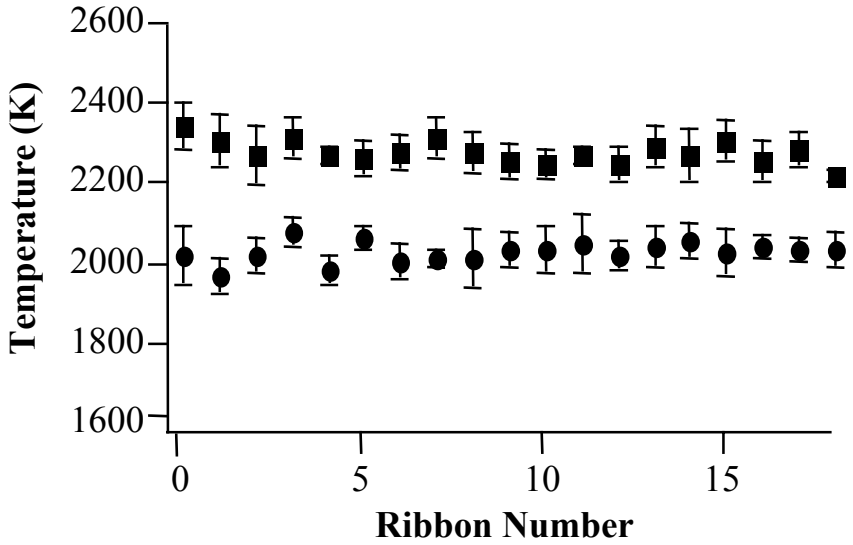

Figure 7. Comparison of temperatures calculated after binning each fiber ribbon individually on the 1-D side of the fiber array. Squares (■) represent temperatures calculated for the acetylene-rich flame and circles (●) represent temperatures calculated acetylene-deficient flame. This shows the vertical temperature distribution.

The temperature distribution for this data can be seen in Figures 8a and 8b for the acetylene-rich and acetylene-deficient flames, respectively. The average temperatures across the whole 2-D side of the array were 2329±153 K and 2090±148 K for the acetylene-rich and acetylene-deficient flames, respectively. This is in agreement with the vertical temperature distribution and average temperature results.

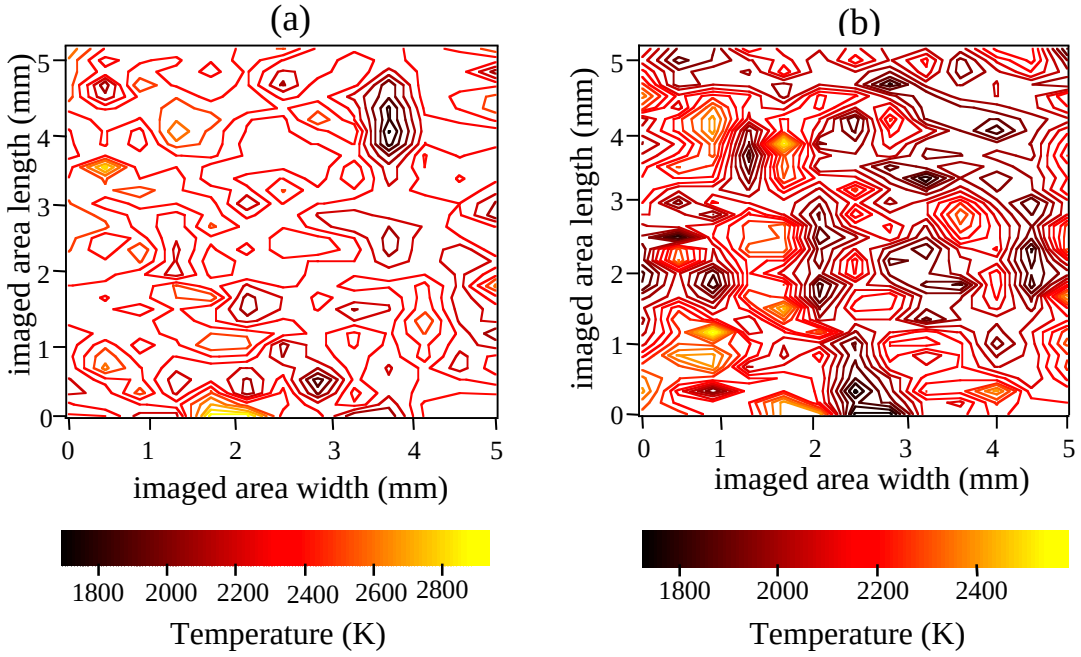

Figure 8 (a) Temperature distribution of an acetylene-rich flame (b) Temperature distribution of an acetylene-deficient flame.

4. CONCLUSION

We have shown that laser ablation is useful for introduction of non-soluble polymer plaques into a flame. We also showed the ability to make temperature "maps" of a flame, simultaneously measuring all points in the imaged area of the flame using a dimension reduction fiber array. This fiber-array technique is generally applicable to any spectral imaging technique.

5. FUTURE WORK

Future work will include determining temperatures in other flame environments. This technique will also be extended to measure the lifetimes and concentrations of •OH, •CH and/or other radical species present in flame environments.

6. ACKNOWLEDGEMENT

This work was supported by the Federal Aviation Administration, FAA Grant No. 95-G-030 and DOE EPSCoR, Grant # EPS9630167.

7. REFERENCES

1. Barden, S.C. ; Scott, K. "The DensePak Fiber Array and Observations," *169th A.A.S. Meeting,* Abstract #30.12, Vol. 18, p.951, Pasadena, 1986.
2. Barden, S.C.; Wade, A.R. "DensePak and Spectral Imaging With Fiber-Optics," in *Fiber Optics in Astronomy*, S.C. Barden Ed., p 113-124, Astronomical Society of the Pacific, San Francisco, CA 1988.
3. Barden, S.C.; Wade, A.R. "Nessie-A Versatile Multi-FiberFeed on the KPNO Mayall 4-Meter Telescope," in *Fiber Optics in Astronomy*, S.C. Barden Ed., p 140-152, Astronomical Society of the Pacific, San Francisco, CA 1988.
4. Parry, I.; Kenworthy, M.; Taylor, K. "SPIRAL Phase A: A Prototype Integral Field Spectrograph for the ATT," in *SPIE Proceedings for the Optical Telescopes of Today and Tomorrow*, Vol. 2871, p. 1325-1331, A.L. Ardeberg Ed., 1997.
5. Haynes, R.; Lee, D.; Allington-Smith, J.; Content, R.; Dodsworth, G.; Lewis, I.; Sharples, R.; Turner, J.; Webster, J.; Done, C.; Peletier, R.; Parry, I.; Chapman, S. *Publ. Astron. Soc. Pac.* **111**, 1451 (1999).
6. Meyer, D.M.; Lauroesch, J.T. *Astrophys. J.* **520**, L103 (1999).
7. Andrews, S.M.; Meyer, D.M.; Lauroesch, J.T. *Astrophys. J.* **552**, L73 (2001).
8. Mclain, B.L.; Ma, J.; Ben-Amotz, D. *Appl. Spec.* **53**, 1118 (1999).
9. Gift, A.D.; Ma, J.; Haber, K.S.; Mclain, B.L.; Ben-Amotz, D. *J. Ramam Spectrosc.* **30**, 757 (1999).
10. Ma, J.; Ben-Amotz, D. *Appl. Spec.* **51**, 1845 (1997).
11. Suto, H. *Infrared Phys. Technol.* **38**, 93 (1997).
12. Nelson, M.P.; Myrick, M.L. *Rev. Sci. Instrum.* **70**, 2836 (1999).
13. Nelson, M.P.; Bell, W.C.; McLester, M.L.; Myrick, M.L. *Appl. Spec.* **52**, 179 (1997).

14. Nelson, M.P.; Myrick, M.L. *Appl. Spec.* **53**, 751 (1999).
15. Schiza, M.V.; Nelson, M.P.; Myrick, M.L.; Angel, S.M. *Appl. Spec.* **55**, 217 (2001).
16. Schiza, M.V.; Nelson, M.P.; Myrick, M.L.; Angel, S.M. "Simple Techniques for Chemical Imaging at Many Wavelengths Simultaneously, Using a Novel 2D to 1D Optical Fiber Array," *in SPIE Proceedings for the Applications of Optical Fiber Sensors*, Vol. 4074, p. 99-107, A.J. Rogers Ed., 2000.
17. Schiza, M.V.; Nelson, M.P.; Myrick, M.L.; Angel, S.M. "Hyperspectral Imaging Sensors Using a Novel 2D to 1D Fiber Array," *in SPIE Proceedings on Fiber-Optic Sensor Technology and Applications,* Vol. 3860, p 317-325, 1999.